A sampled observer for a three-branch supercapacitor model: voltages estimation for SOC under NEDC and WLTP cycles

I. Belghazi[1] and E. Magarotto[2,*] and T. Ahmed-Ali [3] and M. Haddad [4]

***Abstract*— In this paper, we propose an online estimation method for the internal voltages of a three-branch supercapacitor model. The main goal is to provide a fast and accurate estimation of these voltages, which are crucial for assessing the state of charge (SOC) for the management system. To achieve this, we design a decoupled continuous nonlinear observer, whose outputs are discretized using a zero-order hold (ZOH). Simulation results demonstrate that the observer delivers high-performance estimation, even under fast dynamic input conditions, such as those encountered in WLTP cycles.**

***Index Terms*— nonlinear, observer, sampled-data, supercapacitor, three-branch model, WLTP.**

I. Introduction

Optimizing energy storage systems (ESS) is a major challenge in the development of electric vehicles (EVs), renewable energies and embedded systems [1]. Among storage technologies, supercapacitors (SC) stand out for their ability to deliver high power density, high energy efficiency and long life [2], [3]. Unlike lithium-ion batteries, which are limited by electro chemical reactions, supercapacitors store energy in electrostatic form, enabling them to offer faster charge/discharge cycles and a much longer service life [4]. Their integration in Electrical Vehicles (EVs) thus helps to improve battery autonomy, optimize energy recovery during regenerative braking and reduce overall system energy losses [5], [6]. However, effective management of these components is necessary to ensure optimum performance, safety and durability [7], [8].

SC modeling plays an essential role in analyzing their behavior and developing advanced management strategies. Several models exist in the literature, ranging from the simple equivalent RC model to more complex models incorporating internal dynamics. The one-branch model, based on a single RC circuit, is often used because of its simplicity, but it does not accurately capture self-discharge and charge redistribution phenomena [9]. The two-branch model represents a compromise between accuracy and complexity, but is still limited in its ability to represent all the internal dynamics of the SC [10]. Finally, the three branch model is one of the most comprehensive, and can model the different time constants associated with energy transfers in the SC, making it particularly suitable for applications requiring fine estimation of internal states [11].

Estimation of the internal states of SCs relies on algorithms to reconstruct variables inaccessible to direct measurement. Numerous approaches have been developed in the literature: the Luenberger observer is a classical approach based on feedback of measurement errors, but it remains sensitive to uncertainties and disturbances [12]. The Extended Kalman Filter (EKF) is an advanced method capable of handling these uncertainties by linearizing the SC model around the operating point, but this approximation can introduce significant errors, and the algorithm remains computationally expensive [13], [14]. The Unscented Kalman Filter (UKF) offers a better alternative by incorporating a nonlinear transformation of the states, improving the robustness and accuracy of the estimate, but at the cost of increased complexity [15].

More recent approaches aim to improve convergence speed and robustness to perturbations. The high-gain observer (HGO) uses a high observation gain to speed up correction of estimation errors, but it can be sensitive to measurement noise and requires precise parameter tuning [16]. The Generalized Extended State Observer (GESO) is another solution for improving robustness to uncertainties by incorporating on-line identfication of model parameters, guaranteeing better adaptation to SC variations [17]. Finally, sampled observers, such as Zero Order Hold (ZOH), limit the computational load by updating states at discrete instants while maintaining a continuous model between two samples, making them an effective solution for embedded systems [18]. In this paper, we propose the development of a particular observer structure for estimating the internal states of supercapacitors:

- A nonlinear continuous observer, ensuring real-time estimation with exponential convergence of the estimation error.
- A nonlinear sampled Zero Order Hold (ZOH) observer, combining the advantages of discrete and continuous methods to reduce the computational load while maintaining good accuracy.

These kind of observer will be validated by simulation on different input profiles, including constant step charge/discharge cycles, the New European Driving Cycle (NEDC) and the Worldwide Harmonized Light Vehicle Test Procedure (WLTP) cycle. The aim is to compare their performance in terms of estimation accuracy, robustness and computational complexity for efficient integration into supercapacitor man-

[1]I. Belghazi is with CESI-LINEACT, UR 7527, France and with SEGULA Engineering, SEGULA Technologies, 92 500 Rueil Malmaison, France;

[2]E. Magarotto is with NORMANDIE UNIV, 14032 Caen, France;

[*] corresponding author : eric.magarotto@unicaen.fr

[3]T. Ahmed-Ali is with ENSICAEN & CESI-LINEACT, UR 7527, France

[4]M. Haddad is head of R&I Department - SEGULA Engineering, SEGULA Technologies, 9 av. E. Belin, 92 500 Rueil Malmaison, France

agement systems. This paper is organized as follows: Section II presents the system modeling, followed by the design of the nonlinear continuous observer and ZOH observer is presented in Section III. Simulation results are discussed in Section IV, before concluding in last Section.

II. SUPERCAPACITOR CIRCUIT MODEL

A. model discussion

Supercapacitors are generally modeled using equivalent electrical circuit models (ECMs). These models are used to analyze and predict the behavior of supercapacitors prior to their integration into practical applications. The fundamental components of ECMs are resistors and capacitors, which can be combined in series or in parallel to reflect the dynamic characteristics of the supercapacitor. Depending on the desired level of complexity, several types of model exist: some focus on the behavior of the SC during charge and discharge cycles, while others incorporate parameters such as charge/discharge frequency and the evolution of internal characteristics. The most commonly used models include :

- The simple RC model, often supplied by manufacturers, which represents the supercapacitor by an equivalent series resistance (ESR) and a single capacitance. Although suitable for basic applications, this model does not take into account internal phenomena such as load redistribution and the effect of load voltage on capacitance.
- The classic RC(u) model, which improves on the simple model by integrating a variable capacitance dependent on input voltage. However, it remains limited in accuracy over a wide range of frequencies, although it is commonly used to study the ageing of supercapacitors [15].
- The two or three-branch model, which provides a better representation of internal dynamic phenomena by integrating several time constants associated with the charging and discharging processes. The greater the number of branches, the more accurate the model, but at the cost of increased complexity in terms of calculation and parameter identification [19].
- The transmission line model, which seeks to capture charge diffusion in porous electrodes more accurately, although its implementation is more complex and the observation of internal parameters is often treated as a Partial Differentiel Equation (PDE) problem to solve.

The three-branch model used in this study is particularly suited to applications requiring precise energy and temperature management, such as electric vehicles and smart grids. This model is structured into three distinct dynamics:

1) Fast dynamics (*immediate*): corresponding to the initial charging and discharging phases, when energy is mainly stored on the surface of the electrodes.
2) Intermediate dynamics (*delay*): representing energy transfer in the supercapacitor's inner layers.
3) Slow dynamics (*long term*): modeling longer-term phenomena such as self-discharge and charge redistribution [11].

By incorporating effects such as ionic diffusion and electrochemical polarization, the three branch model offers a detailed description of supercapacitor behavior under a variety of conditions. It can therefore be used to better predict performance and optimize energy management strategies in embedded systems. As we use a model-based synthesis for our observer, the accuracy of the chosen model is crucial. The equivalent circuit of the supercapacitor cell is shown in Fig. 1.

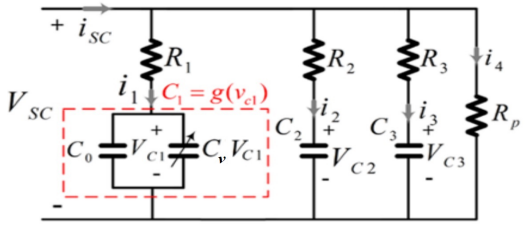

Fig. 1. Three branch model

B. Model equations

As depicted in Fig. 1 :

- V_{sc} is the terminal voltage of the supercapacitor,
- i_{sc} is the input current of the SC,
- V_{c_k} is the internal voltage at each branch k,
- R_1, R_2 and R_3 are the equivalent series resistances,
- R_p is the leakage resistance,
- C_1, C_2, C_3 are the capacitances associated with the three dynamic branches of the SC.

In this model, the capacitance C_1 depends on the voltage and can be approximated as $C_1 = g(V_{c_1})$ a non linear function approximated by $C_0 + C_v V_{c_1}$.

C. State-Space Formulation

Applying Kirchhoff's Current Law (KCL),the expression for the supercapacitor current is obtained as:

$$i_{sc} = i_1 + i_2 + i_3 + i_4 \tag{1}$$

which can be rewritten as:

$$i_{sc} = \frac{V_{sc} - V_{c_1}}{R_1} + \frac{V_{sc} - V_{c_2}}{R_2} + \frac{V_{sc} - V_{c_3}}{R_3} + \frac{V_{sc}}{R_p} \tag{2}$$

After rearrangement, the terminal voltage of the SC is given by:

$$V_{sc} = R_{eq}\left[\frac{1}{R_1}V_{c_1} + \frac{1}{R_2}V_{c_2} + \frac{1}{R_3}V_{c_3} + i_{sc}\right] \tag{3}$$

where R_{eq} represents the overall equivalent resistance of the circuit.

Applying Kirchhoff's Voltage Law (KVL) to each branch:

$$V_{sc} = R_k C_k \frac{dV_{c_k}}{dt} + V_{c_k} \quad k = 1, 2, 3 \tag{4}$$

By substituting (3) into (4),we obtain the system of state-space equations:

$$\begin{aligned}\frac{dV_{c_1}}{dt} = &\frac{(R_{eq} - R_1)V_{c_1}}{R_1^2(C_0 + C_v V_{c_1})} + \frac{R_{eq}V_{c_2}}{R_1 R_2(C_0 + C_v V_{c_1})} \\ &+ \frac{R_{eq}V_{c_3}}{R_1 R_3\,(C_0 + C_v V_{c_1})} + \frac{R_{eq} i_{sc}}{R_1\,(C_0 + C_v V_{c_1})}\end{aligned} \tag{5}$$

$$\frac{dV_{c_2}}{dt} = \frac{R_{eq}V_{c_1}}{R_1R_2C_2} + \frac{(R_{eq}-R_2)V_{c_2}}{R_2^2C_2} + \frac{R_{eq}V_{c_3}}{R_2R_3C_2} + \frac{R_{eq}i_{sc}}{R_2C_2} \quad (6)$$

$$\frac{dV_{c_3}}{dt} = \frac{R_{eq}V_{c_1}}{R_1R_3C_3} + \frac{R_{eq}V_{c_2}}{R_2R_3C_3} + \frac{(R_{eq}-R_3)V_{c_3}}{R_3^2C_3} + \frac{R_{eq}i_{sc}}{R_3C_3} \quad (7)$$

Defining the state variables as:

$$X_1 = V_{c_1}, \qquad X_2 = V_{c_2}, \qquad X_3 = V_{c_3}, \qquad y = V_{sc} \quad (8)$$

the state-space representation of the system becomes:

$$\begin{cases} \dot{X}_1(t) & = \Phi(X,u) \\ \dot{Z}(t) & = AZ(t) + B_0X_1(t) + B_1u(t) \\ y(t) & = d_1X_1(t) + CZ(t) + R_{eq}u(t) \end{cases} \quad (9)$$

with :

$$\Phi(X,u) = [\rho_1 \quad \rho_2 \quad \rho_3]\begin{bmatrix} X_1 \\ X_2 \\ X_3 \end{bmatrix} + \rho_4 \quad u \quad (10)$$

with $\rho_1 = \frac{R_{eq}-R_1}{R_1^2(C_0+C_vX_1)}, \rho_2 = \frac{R_{eq}}{R_1R_2(C_0+C_vX_1)}$, $\rho_3 = \frac{R_{eq}}{R_1R_3\left(C_0+C_vX_1\right)}, \rho_4 = \frac{R_{eq}}{R_1(C_0+C_vX_1)}$.

$Z = \begin{bmatrix} X_2 \\ X_3 \end{bmatrix}$; $X = (X_1;\ Z)$; $A = \begin{bmatrix} \frac{R_{eq}-R_2}{R_2^2C_2} & \frac{R_{eq}}{R_2R_3C_2} \\ \frac{R_{eq}}{R_2R_3C_3} & \frac{R_{eq}-R_3}{R_3^2C_3} \end{bmatrix}$;

$B_0 = \begin{bmatrix} \frac{R_{eq}}{R_1R_2C_2} \\ \frac{R_{eq}}{R_1R_3C_3} \end{bmatrix}$; $B_1 = \begin{bmatrix} \frac{R_{eq}}{R_2C_2} \\ \frac{R_{eq}}{R_3C_3} \end{bmatrix}$; $C = \begin{bmatrix} \frac{R_{eq}}{R_2} & \frac{R_{eq}}{R_3} \end{bmatrix}$; $d_1 = \frac{R_{eq}}{R_1}$

To validate the three-branch model, we used various current profiles representative of real-life supercapacitor applications.

- Constant steps (Charge/Discharge): this basic test, already used in [17], validates the model's response to controlled charge and discharge cycles.
- New European Driving Cycle (NEDC).
- Worldwide Harmonized Light Vehicle Test Procedure (WLTP).

The use of the NEDC and WLTP as current input to our observer enables a more thorough evaluation of the three-branch model under a variety of conditions. This approach ensures that the model is suitable for real-life energy management applications, and facilitates its integration into advanced supercapacitor monitoring systems. Because the SOC depends on the internal voltages which are not directly measurable, an observer is then needed to track them.

III. OBSERVER DESIGN

A. nonlinear continuous observer design

In the literature, classical observers applied to supercapacitors generally use a global approach where the whole model is treated as a single system. However, this approach has its limitations, particularly in terms of computational complexity and stability when multiple dynamics are present. In contrast to the global approaches used in the literature, our method is based on an innovative decomposition of the system into two distinct subsystems:

1) A non linear subsystem X_1 representing the fast dynamics of the supercapacitor,
2) A linear subsystem Z capturing the intermediate and slow dynamics.

This approach simplifies observer design while ensuring improved robustness and accuracy of the estimation.

The nonlinear continuous observer equations are :

$$\begin{cases} \dot{\hat{X}}_1(t) & = \Phi(\hat{X},u) + l_1(y(t)-\hat{y}(t)) \\ \dot{\hat{Z}}(t) & = A\hat{Z}(t) + B_0\hat{X}_1(t) + B_1u(t) + L(y(t)-\hat{y}(t)) \\ \hat{y}(t) & = d_1\hat{X}_1(t) + C\hat{Z}(t) + R_{eq}u(t) \end{cases} \quad (11)$$

with :

$$\Phi(X,u) = [\hat{\rho}_1 \quad \hat{\rho}_2 \quad \hat{\rho}_3]\begin{bmatrix} \hat{X}_1 \\ \hat{X}_2 \\ \hat{X}_3 \end{bmatrix} + \hat{\rho}_4 \quad u \quad (12)$$

with $\hat{\rho}_1 = \frac{R_{eq}-R_1}{R_1^2(C_0+C_v\hat{X}_1)}, \hat{\rho}_2 = \frac{R_{eq}}{R_1R_2(C_0+C_v\hat{X}_1)}$, $\hat{\rho}_3 = \frac{R_{eq}}{R_1R_3\left(C_0+C_v\hat{X}_1\right)}, \hat{\rho}_4 = \frac{R_{eq}}{R_1(C_0+C_v\hat{X}_1)}$.

$\hat{Z} = \begin{bmatrix} \hat{X}_2 \\ \hat{X}_3 \end{bmatrix}$; $L = \begin{bmatrix} l_2 \\ l_3 \end{bmatrix}$.

B. Computation of gains

The gain L is determined by placing desired poles in the observation matrix $(A+LC)$ and L and l_1 must respect constraints obtained by applying the Lyapunov criterion and Young's inequality.

Sketch of proof:

Lets define $\tilde{Z} = Z - \hat{Z}$, $\tilde{X}_1 = X_1 - \hat{X}_1$, $X = (X_1\ Z)$ and $\tilde{X} = (\tilde{X}_1\ \tilde{Z})$.

Define V a Lyapunov candidate function such that:

$$V = V_1 + V_2 \quad (13)$$

$$V_1 = \tilde{Z}^T\ P\ \tilde{Z} \quad (14)$$

$$V_2 = \frac{1}{2}\tilde{X_1}^2 \quad (15)$$

with P respecting $P(A+LC) + (A+LC)^TP \leqslant -\mu I$.

The nonlinear function Φ verify:

$$|\Phi(X,u) - \Phi(\hat{X},u)| \leqslant K|\hat{X} - X| \quad (16)$$

Using Young's inequality, the derivative of V is construct as $\dot{V} = \dot{V_1} + \dot{V_2}$ such that:

$$\dot{V} \leqslant -\beta\ |\tilde{Z}|^2 - \gamma\ |\tilde{X}|^2 \quad (17)$$

with

$$\beta = \left(\frac{\mu}{2} - \frac{2}{d_1}l_1|C|^2\right) > 0 \quad (18)$$

$$\gamma = \left(l_1\frac{d_1}{2} - K - \frac{2}{\mu}|P|^2|B_0 - L\ d_1|^2\right) > 0 \quad (19)$$

$$\mu > 0, d_1 > 0$$

We must ensure that the Lyapunov function derivative satisfies $\dot{V} \leq -\alpha\ V$ which guarantees exponential stability of the estimation error. To determine the gains, L is such that (A+LC) is Hurwitz and l_1 must satisfy inequations (18-19).

C. Sampled-Data observer with Zero-Order Hold (ZOH)

In this section, we introduce a sampled-data observer based on the Zero-Order Hold (ZOH) principle. Unlike continuous-time observers, which update the estimated states in real-time, ZOH-based observers update the state estimates only at discrete sampling instants, while keeping the values constant between two consecutive updates. This approach is particularly useful for digital implementations, where measurements are available at specific sampling times t_k rather than continuously [20].

Motivation for ZOH-Based Estimation:

Many practical applications, especially energy storage management systems, rely on discrete-time sampling due to hardware constraints. While continuous-time observers provide smoother estimations, they are computationally demanding and require real-time feedback, which is not always feasible. On the other hand, ZOH-based observers reduce the computational burden by processing updates at discrete time steps t_k while keeping values between updates.

Mathematical Formulation of the ZOH Observer:

The ZOH observer is governed by the following set of equations:

$$\dot{\hat{X}}_1(t) = \phi(\hat{X}, u) + l_1(y(t_k) - \hat{y}(t_k)) \tag{20}$$

$$\dot{\hat{Z}}(t) = A\hat{Z}(t) + B_0\hat{X}_1(t) + B_1u(t) + L(y(t_k) - \hat{y}(t_k)) \tag{21}$$

$$\hat{y}(t) = R_{eq}\left(\frac{1}{R_1}\hat{x}_1(t) + \frac{1}{R_2}\hat{x}_2(t) + \frac{1}{R_3}\hat{x}_3(t) + u(t)\right) \tag{22}$$

Where $y(t_k)$ represents the measured output at discrete sampling times, $\hat{y}(t_k)$ is the estimated output at these instants and l_1, l_2, l_3 are the observer gains, tuned to ensure stability and convergence.

IV. SIMULATION RESULTS

A. Dynamic load profile: constant steps, NEDC and WLTP

Most simulation procedures use constant step current profiles to clearly distinguish between charging and discharging phases, simplifying the estimation process. However, in the context of electric (EV) and hybrid electric vehicles (HEV), it is more relevant to simulate real-world driving conditions to better assess system performance under dynamic operating conditions [21].

To achieve this, vehicles follow predefined driving cycles, which are speed profiles over time. An ideal driving cycle should meet several key criteria as realism, repeatability and reproducibility,statistical representativeness. Until recently, the NEDC was widely used in the EU for vehicle certification. It is a synthetic driving cycle, mathematically derived, consisting of predefined speed phases, including constant-speed segments and complete stops. However, the NEDC presents some limitations. To overcome these limitations, WLTP was introduced to provide a more realistic assessment of vehicle energy consumption. Compared to the NEDC, the WLTP offers several key improvements such as more aggressive accelerations and decelerations, closer to real-world driving behaviors, a longer driving distance, diverse range conditions (urban, suburban, main roads, and highways) and higher average and peak power demand.

The corresponding current profiles in Fig. 2 are directly derived from the driving cycles and exhibit abrupt discontinuities. These rapid current variations introduce nonlinearities in the system, making the estimation of internal states more challenging. Due to these high dynamic characteristics, many classical observers fail to provide accurate real-time estimates or require significant computational resources, making them less suitable for embedded systems.

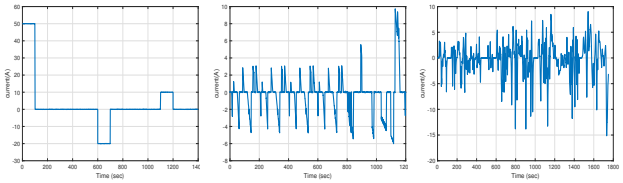

(a) Constant step (b) NEDC (c) WLTP

Fig. 2. Current input profiles

In this work, we applied three profiles presented in Fig. 2 to our observer. Results are presented in Fig. 3 with a focus on first $200s$. For the first current profile Fig. 2a, Applying our observer give similar results to those of [17]. Then, we present only simulations with NEDC and WLTP current input profiles to evaluate the performance of our observers.

B. nonlinear continous observer results

The parameters used correspond to those of the most well-known reference supercapacitor, frequently cited as a standard, as described in [11]. These parameters are summarized in Tab. I.

- Initial conditions for the system model were set to $[U_n\ 0\ 0]$ assuming that the supercapacitor starts in a fully charged state before the NEDC or WLTP test.
- Initial conditions for the observer were set to $[U_n\ 0.01\ 0.01]$ to avoid undesired numerical behavior. The choice of the initial condition of the first state to U_n is made for a better focus of the results. Note that the observer has no problem to exponentialy converge with initial condition 0.01 on the first state.

TABLE I

SUPERCAPACITOR 1500-F THREE-BRANCH PARAMETERS

nominal capacitance	C_{rated}=1500 F	
nominal voltage	U_n=2.7 V	
fast branch	C_0=900 F C_v=300 F/V	R_1=1.5 $m\Omega$
intermediate branch	C_2=200 F	R_2=0.4 Ω
slow branch	C_3=330 F	R_3=3.2 Ω R_p=4 $k\Omega$

To avoid numerical zero inversion and also to test the observer noise robustness, a measurement noise was added to the current profiles before applying them to the model.

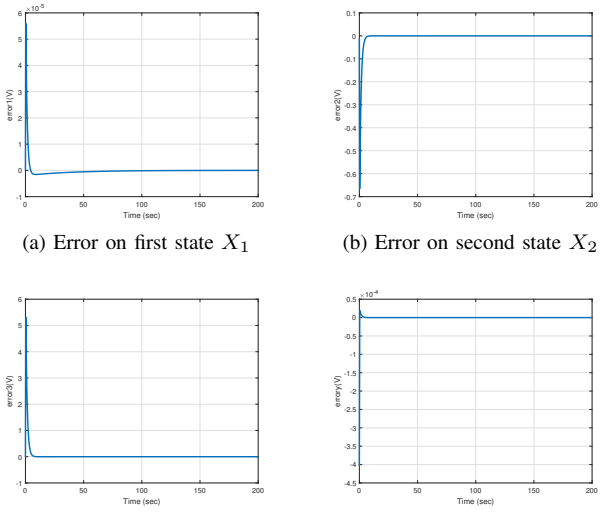

(a) Error on first state X_1 (b) Error on second state X_2

(c) Error on third state X_3 (d) Error on output Y

Fig. 3. Estimation errors (continuous case) with WLTP input

In the continuous case, results for both inputs are very similar. We present only one case (the WLTP one) in Fig. 3.

Without any surprise, the continuous observer is able to adapt effectively to variations in NEDC and/or WLTP cycles, ensuring an accurate and stable estimation of the supercapacitor's internal voltages. The estimation error

converges quickly (in less than a minute), demonstrating its robustness and efficiency for real-time applications. These results are quite obvious because this is a continuous case but they confirms their potential for integration into energy management systems.

C. Sampled-Data Observer with ZOH results

In this subsection, we analyze the (next step) performance of the Zero-Order Hold (ZOH) observer, which has been implemented with a fixed sampling time of $T_e = 0.02s$, the same choice as in [17]. As a natural way, NEDC results in Fig. 4 presents better results than WLTP in Fig. 5. This is a consequence of the highly *nervous* nature and high frequency of the WLTP input.

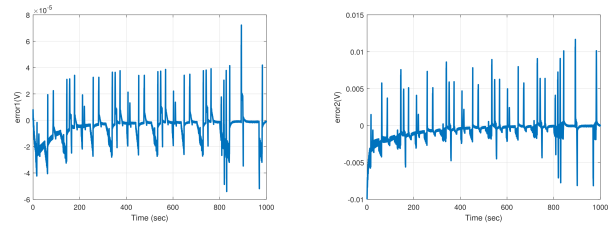

(a) Error on first state X_1 (b) Error on second state X_2

(c) Error on third state X_3 (d) Error on output Y

Fig. 4. Estimation errors (ZOH, $Te = 0.02s$) with NEDC input

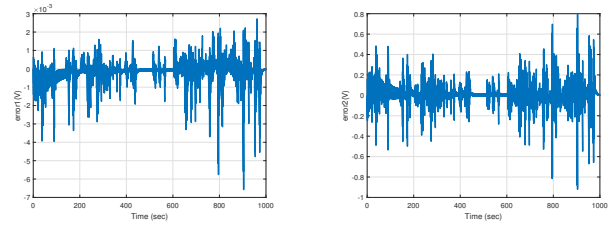

(a) Error on first state X_1 (b) Error on second state X_2

(c) Error on third state X_3 (d) Error on output Y

Fig. 5. Estimation errors (ZOH, $Te = 0.02s$) with WLTP input

remarks: To allow comparisons between NEDC and WLTP, we make the choice to restrict plots time to $1000s$ without any impact on the quality of results because convergence occurs early. Better results can be obtained with a smaller T_e : the smaller the T_e, the smaller the estimation error. We made the choice to not present the better result. The exploration of the better choice of T_e must be made with regards to the specifications. One can note numerous peaks, naturally due to sampling effects. The use of an inter-sampled observer could better this behavior because the estimation would be more accurate between the sampling times and the maximum admissible T_e would be determined.

SOC Results:

One way to calculate SOC is presented in [17]. The definition of the state of charge (SOC) presents many different issues [22]. In general, the SOC is defined as the ratio of the current capacity Q to the nominal capacity Q_n. Then, the SOC can be defined as follows:

$$SOC = \frac{Q}{Q_n} = \frac{(C_0 + C_v V_{C1})V_{C1} + C_2 V_{C2} + C_3 V_{C3}}{Q_n} \tag{23}$$

Then, an accurate estimation of the internal voltages is crucial for the SOC. Simulation results of the SOC and their errors are presented in Fig. 6.

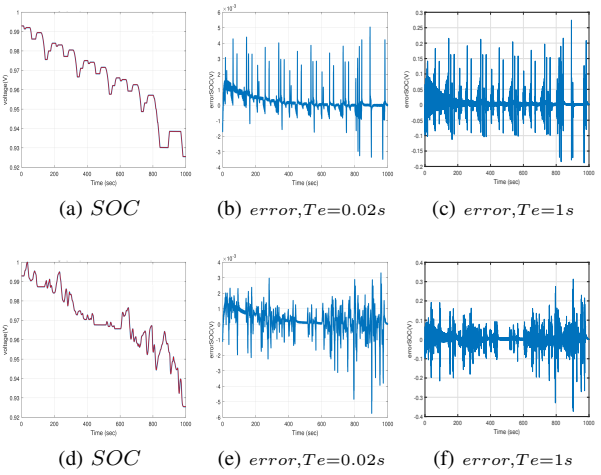

(a) SOC (b) $error, Te{=}0.02s$ (c) $error, Te{=}1s$

(d) SOC (e) $error, Te{=}0.02s$ (f) $error, Te{=}1s$

Fig. 6. SOC and estimation errors of the SOC for $Te = 0.02s$ and $Te = 1s$ with NEDC and WLTP inputs

The results confirm that, despite the discretization, the ZOH observer maintains accurate state estimation, with rapid error convergence. The SOC error estimation is of order 10^{-3} for NEDC and 10^{-3} for WLTP, somehow better than most of results obtain for observer in the literature with constant steps input. Naturally, with $T_e = 1s$, there is a degradation of the estimation accuracy as it is of order 0.2.

If we introduce a kind of RMSE criteria:

$$\lambda = \sqrt{\frac{\sum_0^N (S\hat{O}C_k - SOC_k)^2}{N}},$$

the estimation error of the SOC in terms of root mean square error is shown in the table Tab. II

TABLE II
RMSE FOR SOC

NEDC	$T_e = 0.02s$	$T_e = 1s$
λ	6.3122 e-4	0.0244
WLTP	$T_e = 0.02s$	$T_e = 1s$
λ	7.7382 e-4	0.0364

Using this criteria as index evaluation, NEDC λ value is slightly smaller than WLTP due to the dynamics of the inputs. Results clearly shows that the estimation accuracy is around 40 times better for NEDC and 50 times better for WLTP with a small T_e. Nonetheless, even with a large T_e, we obtain similar results as others works with constant step inputs. This validate our observer and is highly promising in a future use of an inter-sampled observer.

V. CONCLUSIONS

In this paper, we designed a nonlinear sampled-data observer with a particular structure for estimating the internal parameters of supercapacitors, based on a three-branch model. The proposed approach relies on a continuous observer, whose outputs are discretized using a ZOH. This particular structure ensures global exponential convergence of the estimation error, even in the presence of abrupt current variations, such as those encountered in NEDC and WLTP cycles. Simulation results demonstrate the efficiency and robustness of the proposed observer, providing fast and stable estimation of the supercapacitor's internal voltages. These performances confirm its potential for integration into energy management systems for electric vehicles and embedded applications.

Although limited, these results are promising for applying Inter-sampled Observer in future work. This confirms its suitability for applications requiring both real-time performance and stability under varying operational conditions. Then, we plan to extend this study to a hybrid observer with inter-sample prediction, aiming to further enhance real-time estimation accuracy, speed convergence and provide a easy tuning of the desired sampled-time T_e.

ACKNOWLEDGMENT

This research is supported by SEGULA Technologies (9 av. Edouard Belin, 92 500 Rueil Malmaison, France). Thanks for their collaboration and financial support.

REFERENCES

[1] A. El Mejdoubi, A. Oukaour, H. Chaoui, Y. Slamani, J. Sabor, and H. Gualous, "Online supercapacitor diagnosis for electric vehicle applications," *IEEE Transactions on Vehicular Technology*, vol. 65, no. 6, pp. 4241–4252, 2015, doi: 10.1109/TVT.2015.2454520.

[2] J. T. J. Burd, E. A. Moore, H. Ezzat, R. Kirchain, and R. Roth, "Improvements in electric vehicle battery technology influence vehicle lightweighting and material substitution decisions," *Applied Energy*, vol. 283, p. 116269, 2021, doi: 10.1016/j.apenergy.2020.116269.

[3] M. Conte, A. Genovese, F. Ortenzi, and F. Vellucci, "Hybrid battery supercapacitor storage for an electric forklift: A life-cycle cost assessment," *Journal of Applied Electrochemistry*, vol. 44, no. 4, pp. 523–532, 2014, doi: 10.1007/s10800-014-0669-z.

[4] M. Lu, *Supercapacitors: Materials, Systems, and Applications*. John Wiley & Sons, 2013.

[5] S. M. Lukic, S. G. Wirasingha, F. Rodriguez, J. Cao, and A. Emadi, "Power management of an ultracapacitor/battery hybrid energy storage system in an hev," in *IEEE Vehicle Power and Propulsion Conference*, 2006, pp. 1–6, doi: 10.1109/VPPC.2006.4211267.

[6] J. Cao and A. Emadi, "A new battery/ultracapacitor hybrid energy storage system for electric, hybrid, and plug-in hybrid electric vehicles." *IEEE Transactions on power electronics*, vol. 27, no. 1, pp. 122–132, 2011, doi: 10.1109/TPEL.2011.2151206.

[7] J. Park, B. Raju, and A. Emadi, "Effects of an ultra-capacitor and battery energy storage system in a hybrid electric vehicle," SAE International, Technical Paper 2005-01-3452, 2005.

[8] S. Fan, J. Duan, L. Sun, K. Zhang, and Y. Han, "State of charge estimate for super-capacitor based on sliding mode observer," in *IEEE Transportation Electrification Conference and Expo, Asia-Pacific (ITEC Asia-Pacific)*, 2017, pp. 1–5, doi: 10.1109/ITEC-AP.2017.8080946.

[9] F. Naseri, E. Farjah, Z. Kazemi, E. Schaltz, T. Ghanbari, and J.-L. Schanen, "Dynamic stabilization of dc traction systems using a supercapacitor-based active stabilizer with model predictive control," *IEEE Transactions on Transportation Electrification*, vol. 6, no. 1, pp. 228–240, 2020, doi: 10.1109/TTE.2020.2967257.

[10] A. Ayob, S. Ansari, M. S. H. Lipu, A. Hussain, and M. H. M. Saad, "SOC, SOH and RUL estimation for supercapacitor management system: Methods, implementation factors, limitations and future research improvements," *Batteries*, vol. 8, no. 10, p. 189, 2022, doi: 10.3390/batteries8100189.

[11] L. Zubeita and R. Bonert, "Characterization of double-layer capacitors of power electronics applications," *IEEE Transactions on Industry Applications*, vol. 36, no. 1, pp. 199–205, 2000, doi: 10.1109/28.821816.

[12] Y. Zhou, Z. Huang, H. Li, J. Peng, W. Liu, and H. Liao, "A generalized extended state observer for supercapacitor state of energy estimation with online identified model," *IEEE Access*, vol. 6, pp. 27 706 – 27 716, 2018, doi: 10.1109/ACCESS.2018.2837036.

[13] Z. Lei, W. Zhenpo, H. Xiaosang, and D. G. Dorrell, "Residual capacity estimation for ultracapacitors in electric vehicles using artificial neural network," *IFAC Proceedings Volumes*, vol. 47, no. 3, pp. 3899–3904, 2014, doi: 10.3182/20140824-6-za-1003.00657.

[14] A. Hammou and H. Gualous, "Comparative study between high gain observer and extended kalman filter for supercapacitor state of health estimation," in *9th International Conference on Systems and Control (ICSC)*, 2021, pp. 332–337, doi: 10.1109/ICSC50472.2021.9666742.

[15] A. Nadeau, G. Sharma, and T. Soyata, "State-of-charge estimation for supercapacitors : A kalman filtering formulation," in *International Conference on Acoustics, Speech and Signal Processing (ICASSP)*, 2014, pp. 2194–2198, doi: 10.1109/ICASSP.2014.6853988.

[16] A. Nadeau, M. Hassanalieragh, G. Sharma, and T. Soyata, "Energy awareness for supercapacitors using kalman filter state-of-charge tracking," *Journal of Power Sources*, vol. 296, pp. 383–391, 2015, doi: 10.1016/j.jpowsour.2015.07.050.

[17] H. El Fadil, F. Z. Belhaj, A. Rachid, F. Giri, and T. Ahmed-Ali, "Nonlinear modeling and observer for supercapacitors in electric vehicle applications," *IFAC Hosting by Elsevier Ltd*, 2017, doi: 10.1016/j.ifacol.2017.08.262.

[18] F. Naseri, S. Karimi, E. Farjah, E. Schaltz, and T. Ghanbari, "Co-estimation of supercapacitor states and parameters considering three-branch equivalent circuit model," in *11th Power Electronics, Drive Systems, and Technologies Conference (PEDSTC)*, 2020, doi: 10.1109/PEDSTC49159.2020.9088356.

[19] E. Magarotto, T. Ahmed-Ali, and M. Haddad, "An hybrid observer for a two-branch supercapacitor model : voltages estimation for SOH and SOC under NEDC and WLTP cycles," in *10th IEEE Conference on Control Decision and Information Technologies, La Vallette, Malta,*, 2024, pp. 1028–1033, doi: 10.1109/CoDIT62066.2024.10708190.

[20] T. Ahmed-Ali, L. Burlion, F. Lamnabhi-Lagarrigue, and C. Hann, "A sampled-data observer with time-varying gain for a class of nonlinear systems with sampled-measurements," in *53rd IEEE Conference on Decision and Control*, 2014, pp. 316–321, doi: 10.1109/CDC.2014.7039400.

[21] E. Giakoumis, *Driving and Engine Cycles*. Springer Cham, 2017, doi: 10.1007/978-3-319-49034-2.

[22] N. Watrin, B. Blunier, and A. Miraoui, "Review of adaptive systems for lithium batteries state-of-charge and state-of-health estimation," in *IEEE Transportation Electrification Conference and Expo (ITEC)*, 2012, pp. 1–6, doi: 10.1109/ITEC.2012.6243437.